REVIEW OF RECENT BALLISTIC RANGE BOUNDARY-LAYER

TRANSITION WORK ON ABLATING BODIES AT AMES

By Thomas N. Canning, Michael E. Tauber, and Max E. Wilkins

Ames Research Center, NASA
Moffett Field, California 94035

INTRODUCTION

To assess the possibility of achieving extensive laminar flow on
low-fineness-ratio cones during hyperbolic entry, the Ames Research
Center is investigating boundary-layer transition on ablating cones.
Results are presented here of ballistic range experiments with models
that ablated at dimensionless mass transfer rates comparable to those
expected for real flights at speeds up to 17 km/sec (56,000 fps). Pre-
liminary results of this study have been published in references 1-3.
The early data (refs. 2 and 3) consisted mainly of measurements of the
total ablated mass; these were compared with the mass that should have
been removed by either fully laminar or fully turbulent flow. The data
all fell between these extremes and showed a reasonable progression
toward the turbulent theory as the area of the model covered with clearly
discernible, roughly triangular regions of increased mass removal
(turbulence wedges) increased. While this correlation seemed to give
a reasonable indication of the nature of the boundary-layer flow
during ablation, several Delrin models, launched at more than 5 km/sec
with no perceptible turbulence wedges, inexplicably lost more mass
than predicted by laminar theory (refs. 2 and 3).

Subsequent to the publication of reference 3, it was found possible to measure the surface recession accurately enough to identify laminar, transitional, and turbulent flow along generators of the recovered cones. The improved method of interpreting data is used in the present paper.

In addition to the improved measurements of mass removal, the present paper updates the microscopic studies of the recovered bodies and more completely describes the surface markings eroded into them. Further, a possible relationship is noted between the observed markings and strong streamwise vortices in boundary layers found by other investigators.

FACILITY AND EXPERIMENTS

Models, 30° half-angle plastic cones with 1-cm base diameters, were launched in free flight in air at a static pressure of 1 to 3 atm. The launch velocities ranged from 2.2 to greater than 7 km/sec, corresponding to free-stream Mach numbers from 7 to 21 and local Reynolds numbers, based on slant length, of 3 to 20 million. Following launch, the cones experienced initially high convective heating and high ablation rates; however, because of their low density and high drag, the models decelerated rapidly to subsonic speeds within about 30 m and flew into an open cylindrical "catcher" tunnel alined with the flight path. The models came to rest in the tunnel and were then recovered. (The purpose of the tunnel was to prevent the models from veering off course and damaging themselves by striking equipment within the range.)
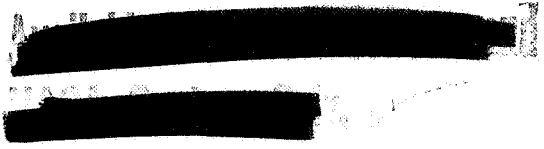
The first 18 m of the ballistic range is instrumented with seven

shadowgraph stations in orthogonal planes,while the tunnel occupies

the last two-thirds of the 67-m-long range. Cones recovered in this

manner have a remarkably large portion of their surfaces undamaged

by impact in the catcher.

The model materials had to be strong enough to withstand the

extreme launch accelerations and low densities to allow aerodynamic

deceleration to low velocities within the available distance. On

this basis, two plastics, Lexan and Delrin, were used.

Analysis of Recovered Bodies

The recovered bodies were photographed extensively with an optical

comparator at 20 power magnification to obtain accurately scaled

profiles along the cone generators. (Profiles were recorded before

the tests as well.) The changes in profile reveal the local integrals

of mass-loss rate during flight. On meridians where the mass loss

varied inversely as the square root of distance from the original

apex, the observed loss was minimal; therefore, the flow was con-

sidered to be essentially all laminar. On other meridians, the

profiles of mass loss showed lengthwise variations, which suggest

transitional and fully turbulent flows. The conclusions drawn from

these profiles regarding the occurrence of transition are more

reliable than those based on the overall mass-loss measurement.

In addition to the quantitative data from the profiles, a wealth

of qualitative and some quantitative information has been gleaned from

an extensive photomicrographic study of the ablated surfaces. The methods of microscopy include exterior and interior illumination with various light sources and different viewing modes, that is, surface interferometry, oblique-wire-shadow and normal view with varying focus position. The patterns formed in the bodies are of necessity related to periodic temporal or steady spatial variations in the boundary-layer structure which may actually be stabilized by the sculpturing they produce.

RESULTS AND DISCUSSION

While the profile data are most useful in defining the type of boundary-layer flow responsible for the various patterns, the patterns themselves may also be useful insofar as they may represent peculiar features of the boundary layer responsible for their production. To this end, the geometric characteristics of the patterns are described below in the context of the boundary layers thought to be responsible for their production. Recognition of features of this sort may eventually lead to a better understanding of the physical processes occurring within the boundary layer.

The wide variety of surface markings complicates the discussion of the surface-recession data. The profiles across distinctive features will be presented and compared with one another when possible. Longitudinal and lateral periodicity in the surface markings will be related, whenever possible, to the flight conditions or other test parameters. In both cases the observations will be related as completely as possible to those published earlier.

Surface Features

The surface features of the ablated models have already been discussed briefly and illustrated in references 1-3. (The very presence of the patterns suggests that they may stabilize the position of inhomogeneities.) An effort will now be made to expand the earlier remarks and present quantitative descriptions that relate the patterns to the test conditions whenever possible.

Features behind roughness elements.- The triangular areas of increased ablation formed behind single elements of three-dimensional roughness (e.g., fig. 1), described in references 1-3, appear to correspond directly to patterns on flat plates found many years ago by Gregory and Walker (ref. 4) and Korkegi (ref. 5) in subsonic and supersonic flow, respectively, and on cones in supersonic flow by Van Driest and McCauley (ref. 6). Initially, the wedge grows slowly, suggesting that the flow is still basically laminar, although the deep grooves behind the roughness element indicate the presence of strong longitudinal vortices. The increase in wedge angle farther downstream is probably caused by intermittent or steady turbulent flow; the longitudinal vortices persist, however. (The similarity between the turbulence wedges of references 4-6 and the present ones is remarkable in view of the wide range of conditions, that is, flat plate and cones of different angles, and Mach numbers and pressures two orders of magnitude greater than those of reference 4, for example.)

The resemblance of the pattern of streamwise grooves in the present models and the drying patterns and flow visualization photographs

in reference 4 is apparent. Unanswered is the question of whether grooves represent the traces of single vortices as indicated in reference 4 or whether they are produced at the influx boundary between two counterrotating vortices (no groove or perhaps a ridge formed at the efflux boundary between opposite-handed pairs). The analysis of Persen (ref. 7) suggests the latter.

Also, it is perhaps significant that the spacing of the longitudinal grooves about one-third the length of the wedge from the roughness element (fig. 1) is greater than the spacing twice as far aft. New grooves were probably formed; the outer grooves appear to diverge more rapidly than cone generators.

The clear, somewhat hyperbolic curve in this figure has been termed a "hyperbolic front." Its significance is unclear; it is frequently found downstream of single spots of roughness on Lexan bodies and vestiges are occasionally discernible on Delrin surfaces.

Wavy Grooves or Crosshatching

The most baffling pattern (fig. 2), only recently discovered, at first glance looks like crosshatching produced by grooves passing spirally in both directions over the surface. The pattern actually consists of many wavy longitudinal grooves such as shown on two of the recovered models at three magnifications. The model of figure 2(a) was launched at 6.3 km/sec through 2 atm air; at a maximum local Reynolds number of 12.2 million, its mass-loss fraction was large enough to indicate turbulent flow throughout most of the flight. A similar pattern, which differs in detail, but was probably produced

by the same boundary-layer process, is shown in figure 2(b). The
model in figure 2(b), fired at 3.7 km/sec, at 2 atm, Re_ϵ = 8 million,
experienced a mass loss and surface recession compatible with laminar
flow, but is thought to have had turbulent flow at low supersonic speeds,
where the local Reynolds number was still high enough to permit transi-
tion. The local shear was great enough to "mold" the melt layer, but
not to remove material.

The sizes and shapes of the patterns are described below and are
related to the conditions under which they were formed. Since neither
the actual flow details responsible for the patterns nor the condi-
tions during flight when the patterns are actually established are
known, the observations are related to the ambient atmosphere and the
launch speed. (Note that surface static pressure and dynamic pressure
are directly proportional to range pressure.)

The wavelength of the wavy patterns for Lexan and Delrin bodies
at four different ambient pressures is given in figure 3. (The
wavelength is almost independent of body station.) The shorter wave-
length at high pressure suggests a relationship to the boundary-layer
skin friction, and the lack of significant longitudinal variation
suggests independence of the boundary-layer thickness. Two of the
three cases shown for an ambient pressure of 1 atm (Lexan) had arti-
ficial roughness (i.e., the diamond and circle symbols indicate screw
threads of 0.016 mm and 0.035 mm advance per thread, respectively).
The thread pitch did not influence the groove wavelength because the
pitch is so fine. Further, it is concluded, tentatively, that the
difference attributable to pressure change is unaffected by the very
fine grooves on those models tested at lower pressure.

The width-to-length ratio (around 0.6) of the patterns is fairly

independent of position and pressure. The size of the patterns does

not grow as rapidly as the girth of the cone; therefore, new grooves

must have started occasionally at scattered points within the pattern.

A careful search of many photographs reveals numerous irregularities

in the overall regular pattern which can be interpreted as the forma-

tion of new grooves. Some of these survive, many appear to decay.

The crosshatching has formed on many bodies tested in the

ballistic range, in the HT 156 burner facility at Manned Spacecraft

Center (Teflon cone), and on 30° half-angle ablating cones of camphor

and of Lucite tested in the Ames 3.5-Foot Hypersonic Wind Tunnel

by H. Larson and G. Mateer and elsewhere. Similar-appearing patterns

have been found in the sand on beaches after wave recession. The

standing-wave patterns in shallow streams flowing over sandy bottoms

also resemble the gross features noted above.

Surface Wavelets

Almost all recovered Lexan models have an overlay of very fine

wavelets, roughly normal to the local flow direction (see fig. 1).

The average wavelengths of these wavelets have been studied in a cur-

sory manner. Averages over small areas were used because of large

local variations. There appears to be sufficient order in the

findings to warrant their inclusion here.

There is no orderly trend of observed wavelength with initial

flight speed. The mean length observed 3 mm from the nose appears

to decrease with increasing ambient pressure, as shown in figure 4.

A hyperbola is included in this plot to suggest a possible inverse variation of wavelength with laminar skin-friction shear. The wavelength is almost invariably shorter near the base than at the 3 mm station (it is longer in only 2 cases in 15) and the variation of wavelength on any one model among several models is far greater at the 9 mm station than at the forward station. This suggests laminar-to-turbulent transitional flow during the time when the surface froze.

Surface Recession

The appearance of the surfaces, discussed above, may aid in the further understanding of boundary layers. The actual ablation produced at these features indicates the relative importance of the phenomena responsible. First, measurements of surface recession will be shown for models with no surface indications of turbulence, that is, wedges. Then, surface-recession profiles across the other (previously discussed) features will be presented.

A number of Delrin models launched at more than 5 km/sec had no visible turbulence wedges, yet they lost substantially more mass than predicted by laminar theory (refs. 2 and 3). It was decided to try to measure the surface recession from ablation along cone generators. Despite the difficulties of measuring changes of 0.1 to 0.01 mm because of the inherent errors introduced by the lack of reliable reference points on the models, the shape of the profile curves shows either the distinct inverse-square-root

variation with distance characteristic of laminar ablation or the significant deviations from this behavior expected if the flow is transitional or turbulent. Fairly typical loss profiles, taken on the same body along two rays 180° apart (fig. 5), are compared with theoretical estimates for fully laminar and fully turbulent flow. Clearly, one ray had fully laminar flow while the other was transitional and turbulent at least part and possibly most of the time. Interestingly, the turbulent ablation pattern suggests a body-fixed transition; in contrast, a transition point moving in an orderly manner as the model slows down, with ever decreasing Reynolds number, would produce a concave ablation profile with maximum mass removal at the base. Other models with turbulent flow outside the wedges, as deduced from profile measurements, also appeared to have had body-fixed transition. It is possible that minute roughnesses that caused the transition were subsequently removed by ablation so that no obvious surface imperfection could be found.

Next, three profiles on a Delrin model with turbulence wedges are shown in figure 6. Surface recession is shown for the 0° generator (defined as the centerline of a large turbulence wedge) and also for a ray about 5° off the wedge centerline originating at the model nose. Note that near the front of a narrow wedge (such as shown in fig. 1) the profile measurement shows the edge of the wedge rather than the bottom. Noteworthy is the comparison of the surface recession along the 0° ray with the turbulent theory; the measured value at the 0.71 body station is 25 percent above the theory and remains 15 to 20 percent above. (The overshoot may be due to an incorrect choice of the effective origin of turbulence; in the theoretical computation

the model nose was considered to be the origin. The reference
enthalpy method was used to compute the turbulent heating (as used
in NASA TR R-185).) Since the turbulent theory is generally somewhat
above the data (see figs. 6 and 7, ref. 2), the intense heating along
the centerline of the wedge in figure 6 may have been intensified by
the persistence of strong longitudinal vortices within the turbulent
region (an observation previously noted). Caution should be exercised,
however, with the surface-recession-measurement results because of the
previously mentioned uncertainty in reference points for the measurements.

The profiles shown are for the Lexan model which was used to
illustrate the wavy grooves in figure 2(a). The surface-recession
profile of the model along two rays 180° apart is shown in figure 7; the
surface along both rays was covered with wavy grooves starting at
the indicated body stations. The profiles indicate that turbulent
flow predominated in the region where the wavy grooves appeared; also,
the profiles again suggest that transition was fixed relatively far
forward.

CONCLUDING REMARKS

The results of the present study further document earlier
descriptions which suggested that a remarkable degree of order exists
in turbulent boundary-layer flows. The straight and wavy streamwise
grooves found in the recovered models attest to this order and may
have aided in stabilizing the position of the boundary-layer
nonuniformities themselves.

Profiles of mass removal over crosshatched areas (wavy grooves) indicate the flow to be transitional or fully turbulent. Most profiles across turbulence wedges were similar; however, one profile at the centerline of one wedge showed greater mass removal than predicted by turbulent theory, assuming the effective turbulent origin to be at the model nose.

Because the models were so small, roughness was frequently the cause of transition. The highest observed local Reynolds number of laminar flow was greater than 8 million at an edge Mach number of about 4. The corresponding boundary-layer displacement-thickness Reynolds number was about 3000; ablation in this case increased the displacement thickness about 25 percent.

SYMBOLS

m	mass of body
m_o	mass of body at launch
p_∞	ballistic-range static pressure
r	body radius
r_b	body base radius
Re_ϵ	maximum local Reynolds number based on boundary-layer edge properties at launch
V_o	launch velocity
x	body slant length measured from original apex
x_b	total body slant length

REFERENCES

1. Wilkins, Max E.: Evidence of Surface Waves and Spreading of Turbulence on Ablating Models. AIAA J., vol. 3, 1965, pp. 1963-1966.

2. Wilkins, Max E.; and Tauber, Michael E.: Boundary-Layer Transition on Ablating Cones at Speeds up to 7 km/sec. AIAA J., Aug. 1966, pp. 1344-1348.

3. Canning, Thomas N.; Wilkins, Max E.; and Tauber, Michael E.: Boundary-Layer Phenomena Observed on the Ablated Surfaces of Cones Recovered After Flights at Speeds up to 7 km/sec. Presented at the Specialists' Meeting of the Fluid Dynamics Panel of AGARD, Colorado State Univ., Fort Collins, Colorado, May 1967.

4. Gregory, N.; and Walker, W. S.: The Effect on Transition of Isolated Surface Excrescences in the Boundary Layer. Rep. and Memo 2779, British ARC, 1956.

5. Korkegi, R. H.: Transition Studies and Skin-Friction Measurements on an Insulated Flat Plate at a Mach Number of 5.8. IAS J., vol. 23, 1956, pp. 97-107.

6. Van Driest, E.; and McCauley, W. D.: The Effect of Controlled Three-Dimensional Roughness on Boundary-Layer Transition at Supersonic Speeds. Rep. MD59-115, North American Aviation, Nov. 1958. AFOSR TN-58-176, AD152-209.

7. Persen, Leif N.: A Simplified Approach to the Influence of Goertler-Type Vortices on the Heat Transfer From a Wall. ARL 65 88, Norges Tekniske Hoegskole, Trondheim, Inst. for Mekanikk, May 1965.

FIGURE CAPTIONS

1. Turbulence wedge on Lexan model.

2. Two crosshatched patterns on Lexan models at three magnifications.

    (a) V_O = 6.3 km/sec

    (b) V_O = 3.7 km/sec

3. Variation of wavelength of wavy grooves with ambient pressure.

4. Variation of average wavelength of surface wavelets with ambient pressure.

5. Surface-recession profiles of Delrin model with no wedges.

6. Surface-recession profiles of Delrin model with turbulence wedges.

7. Surface-recession profiles of Lexan model with wavy grooves.

ROUGHNESS ELEMENT

LONGITUDINAL
GROOVES

HYPERBOLIC FRONT

0

.5 mm
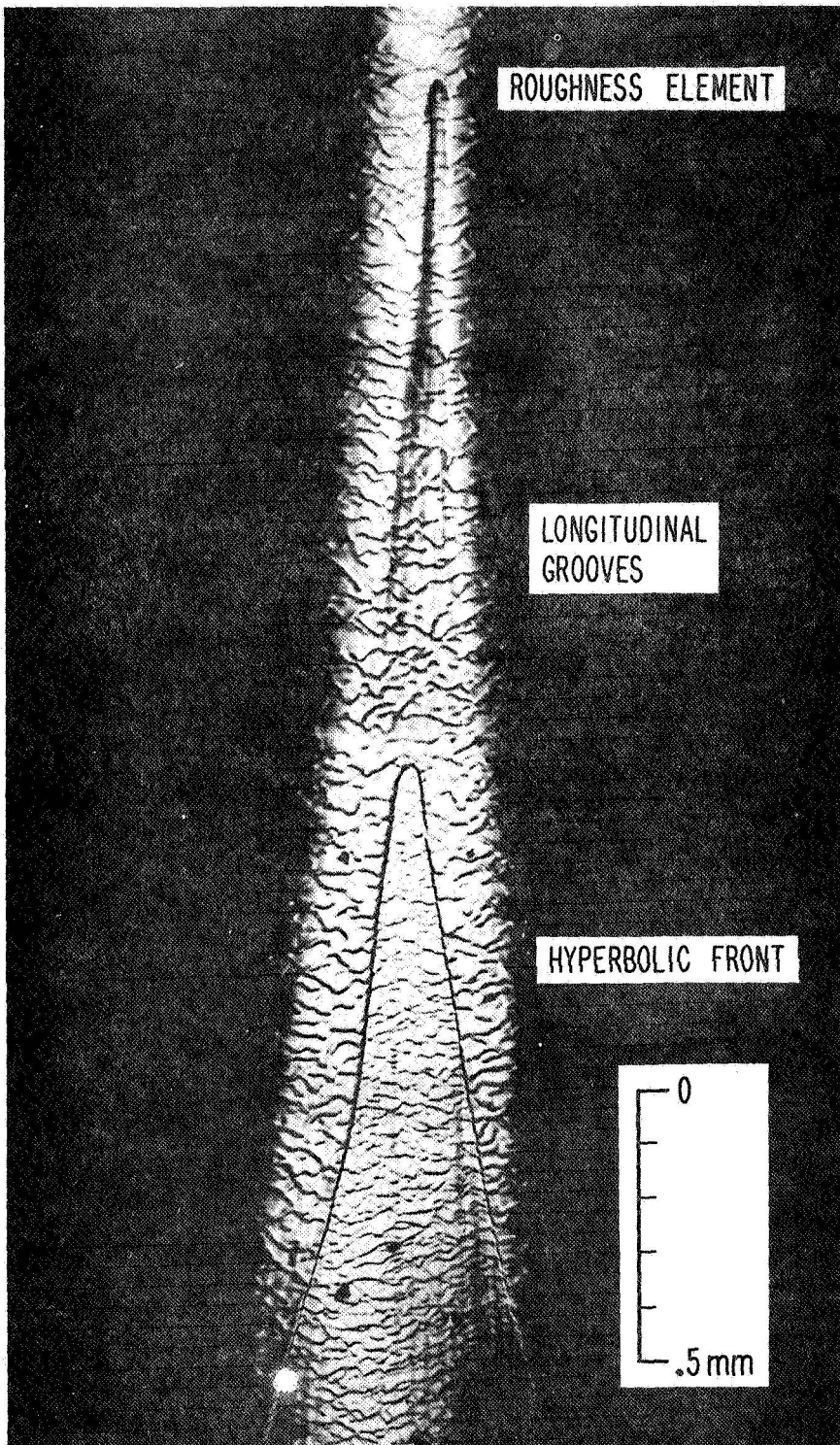
Figure 1.- Turbulence wedge on Lexan model.

FLOW

.1 mm

.2 mm

.4 mm

$V_O = 6.3$ km/sec

$V_O = 3.7$ km/sec

(a) $V_O = 6.3$ km/sec
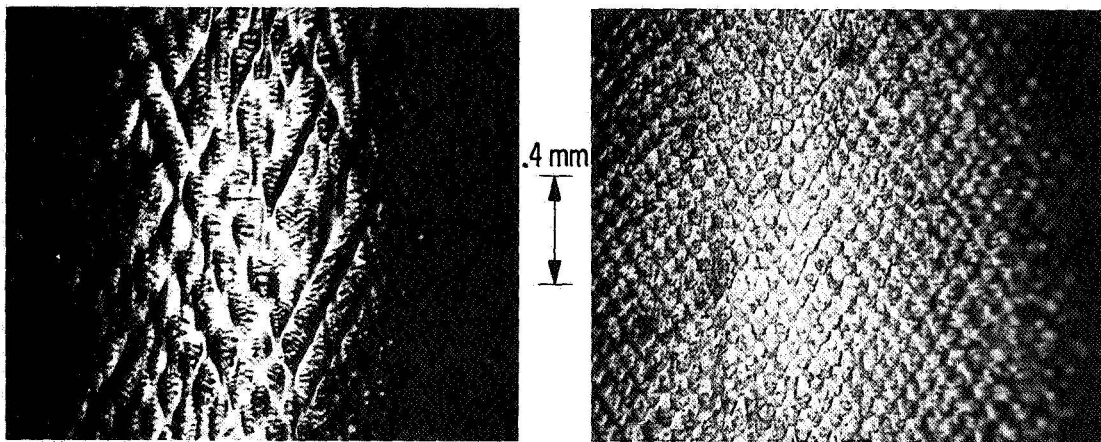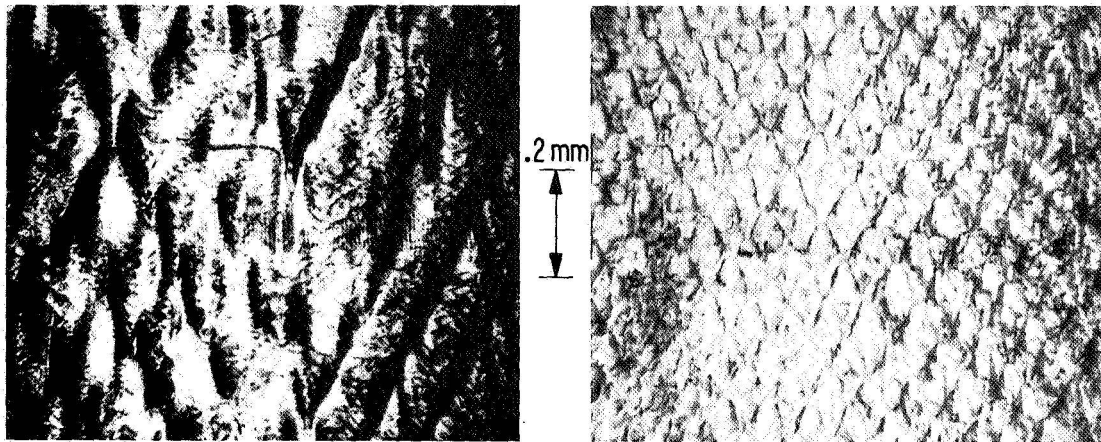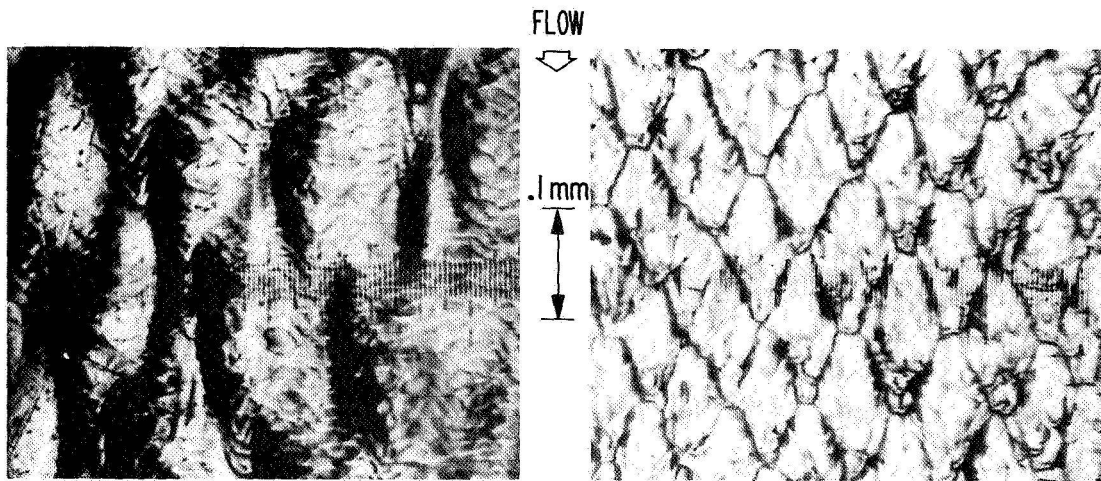
(b) $V_O = 3.7$ km/sec

Figure 2.- Two crosshatched patterns on Lexan models at three magnifications.
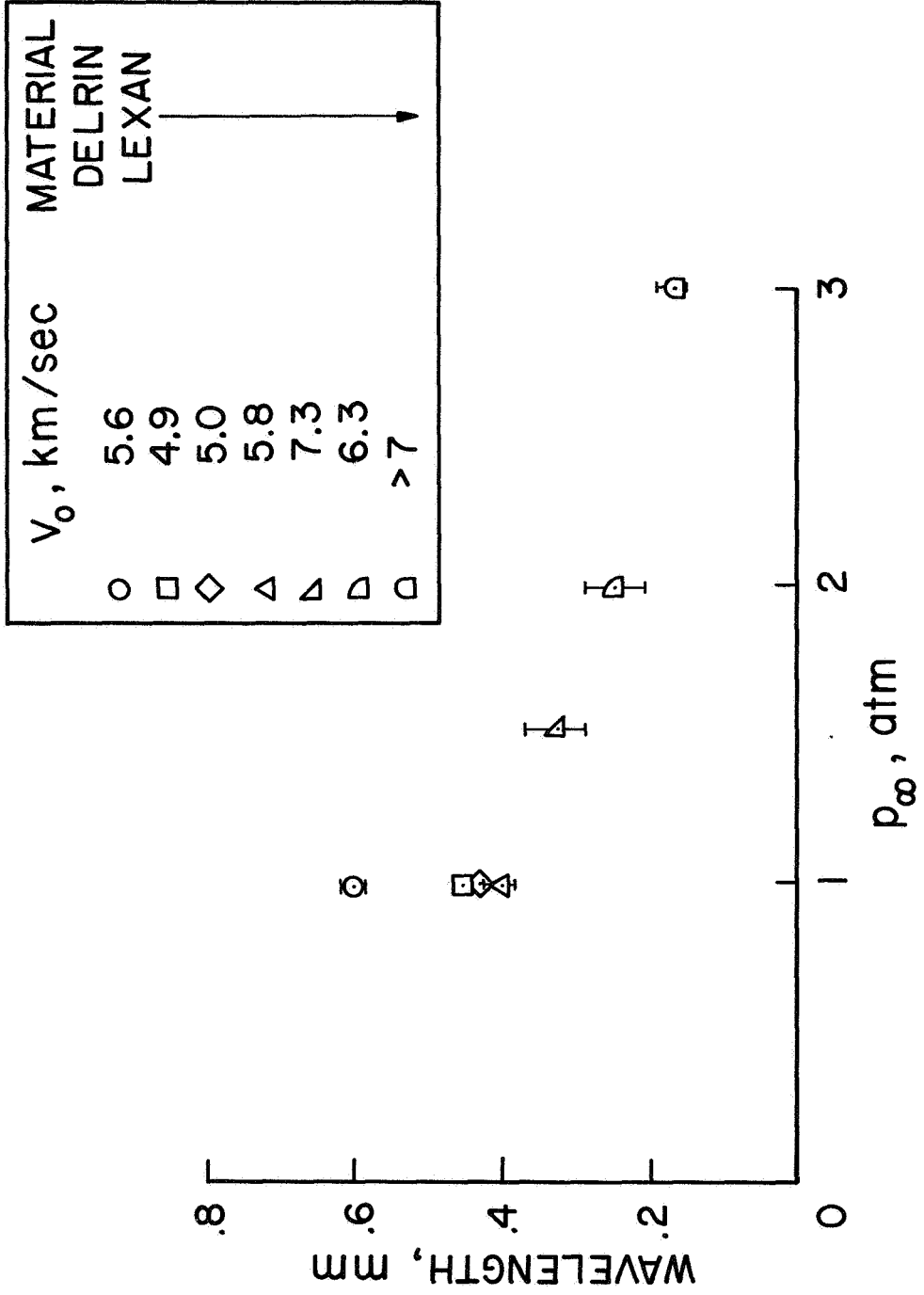
Figure 3.- Variation of wavelength of wavy grooves with ambient pressure.
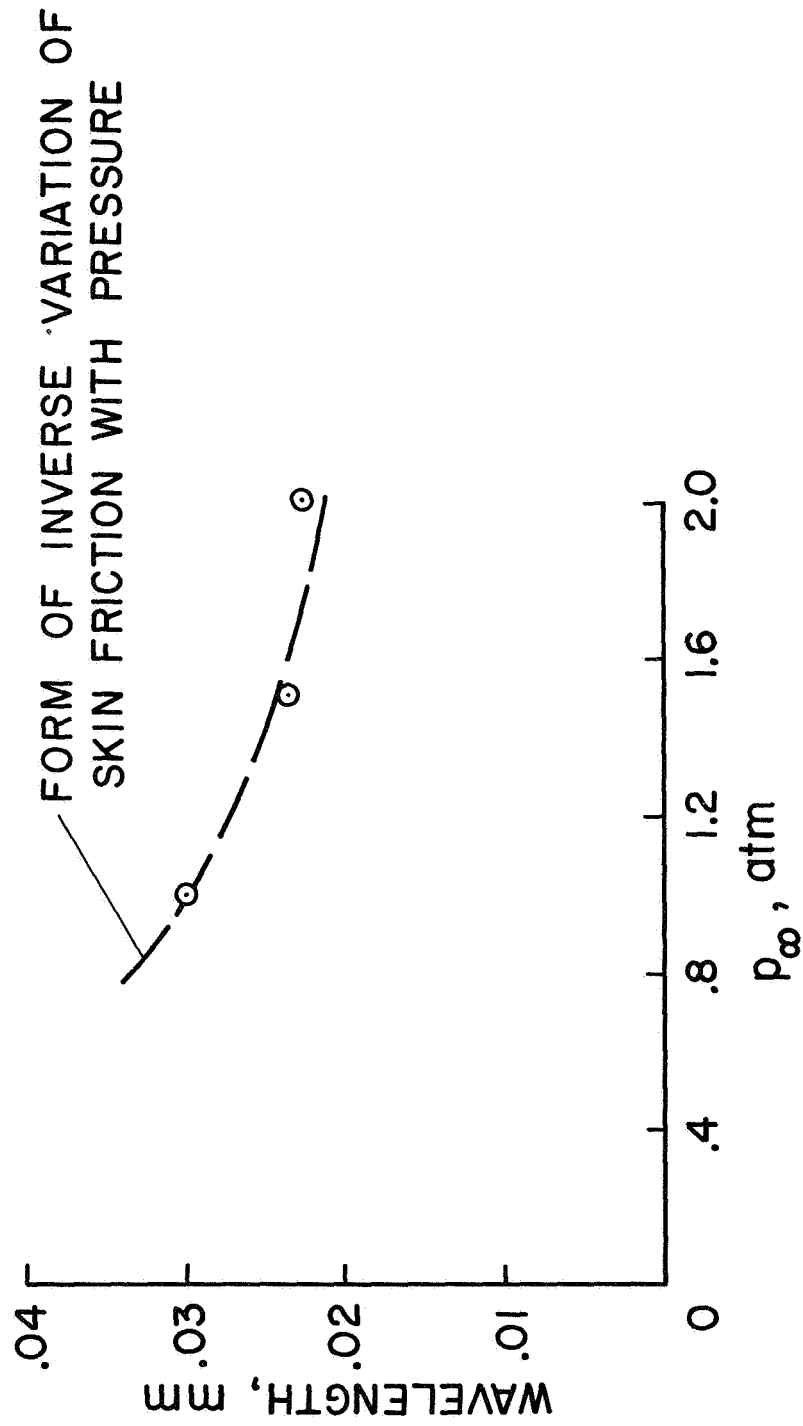
Figure 4.- Variation of average wavelength of surface wavelets with ambient pressure.
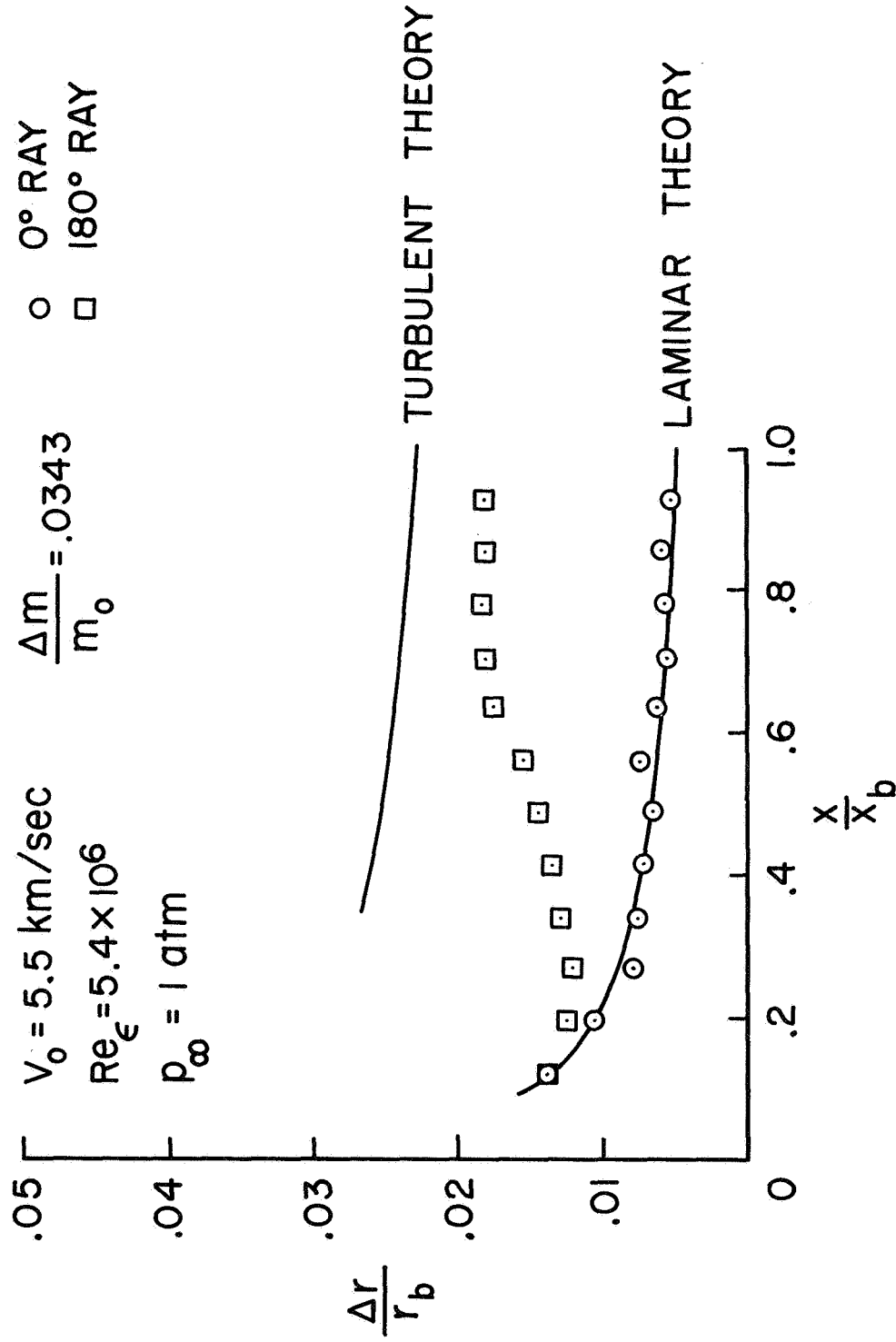
Figure 5.- Surface recession profiles of Delrin model with no wedges.

$V_0 = 5.3$ km/sec

$Re_\epsilon = 5.3 \times 10^6$

$\dfrac{\Delta m}{m_o} = .0380$

$p_\infty = 1$ atm

$\bigcirc$ ¢ OF WEDGE - 0° RAY

$\triangle$ 5° OFF WEDGE ¢

(ORIGIN AT MODEL NOSE)
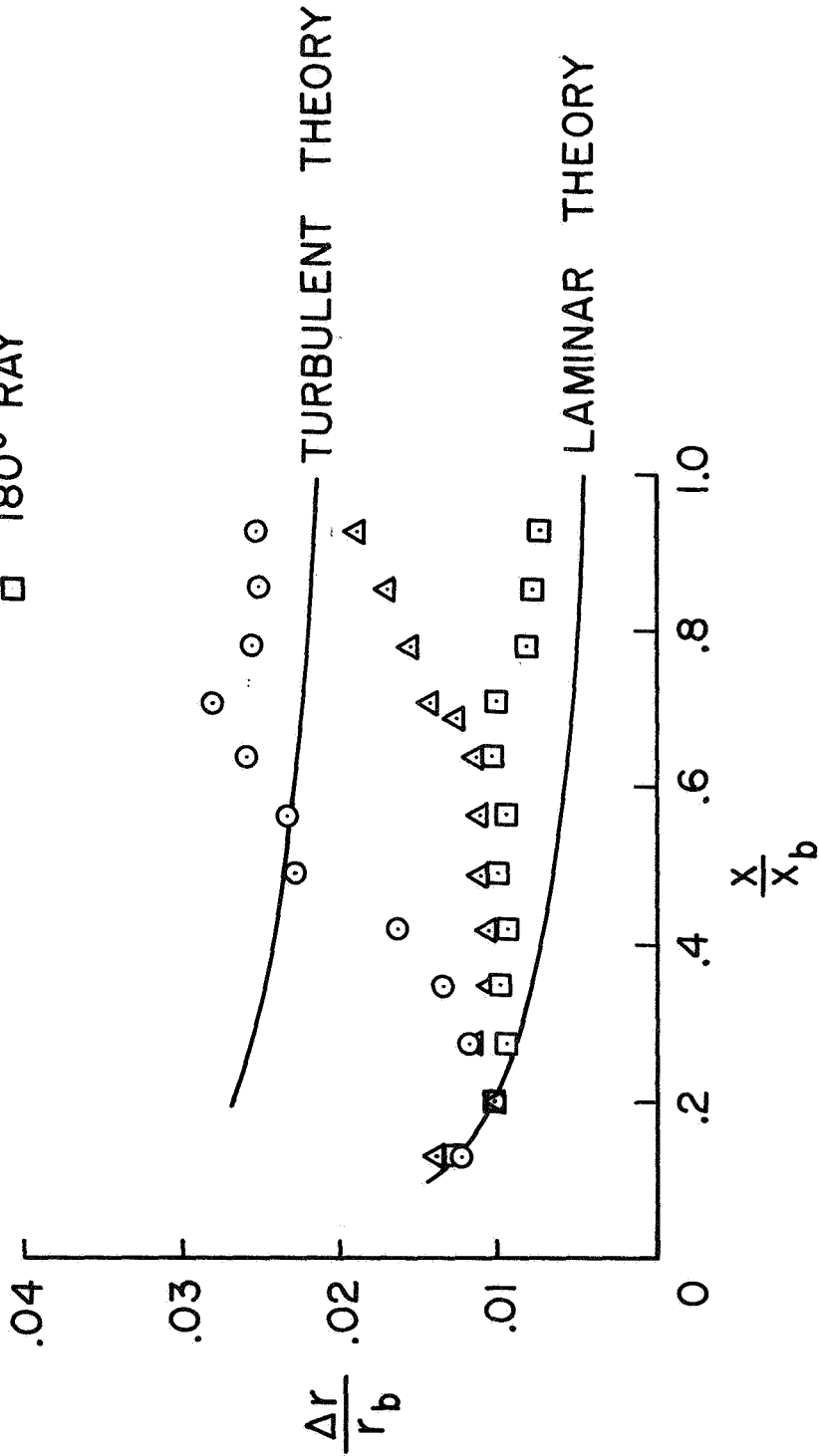
$\square$ 180° RAY

TURBULENT THEORY

LAMINAR THEORY

$\dfrac{\Delta r}{r_b}$

.04

.03

.02

.01

0

.2   .4   .6   .8   1.0

$\dfrac{x}{x_b}$

Figure 6.- Surface recession profiles of Delrin model with turbulence wedges.
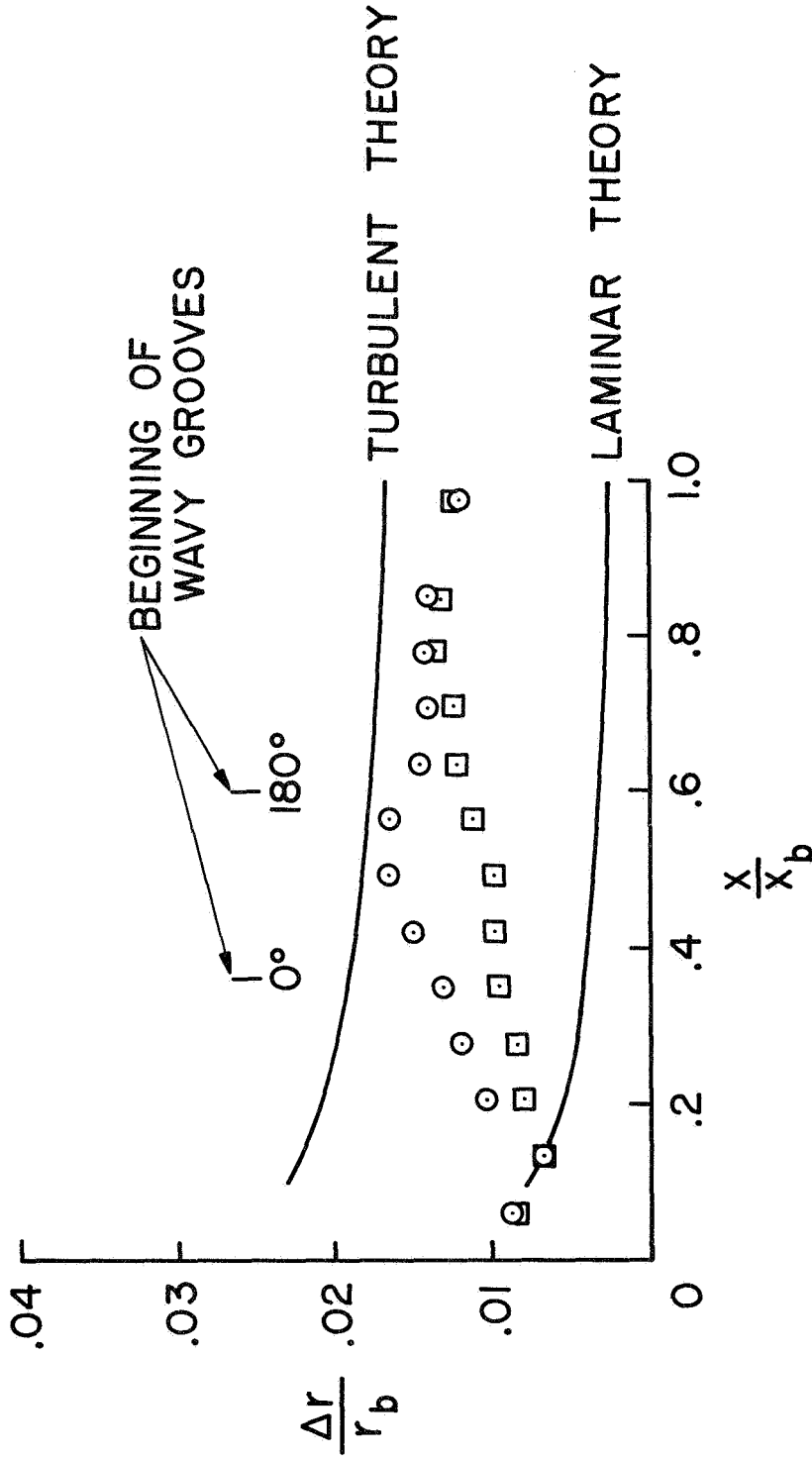
Figure 7.- Surface recession profiles of Lexan model with wavy grooves.